Supplementary Data

BIOENGINEERING ANABOLIC VITAMIN D-25-HYDROXYLASE ACTIVITY INTO THE HUMAN VITAMIN D CATABOLIC ENZYME, CYTOCHROME P450 CYP24A1, BY A V391L MUTATION

Martin Kaufmann[1], David E. Prosser[1], Glenville Jones[1,2]
Departments of Biochemistry[1] and Medicine[2],
Queen's University, Kingston, Ontario, Canada K7L 3N6

Contents:

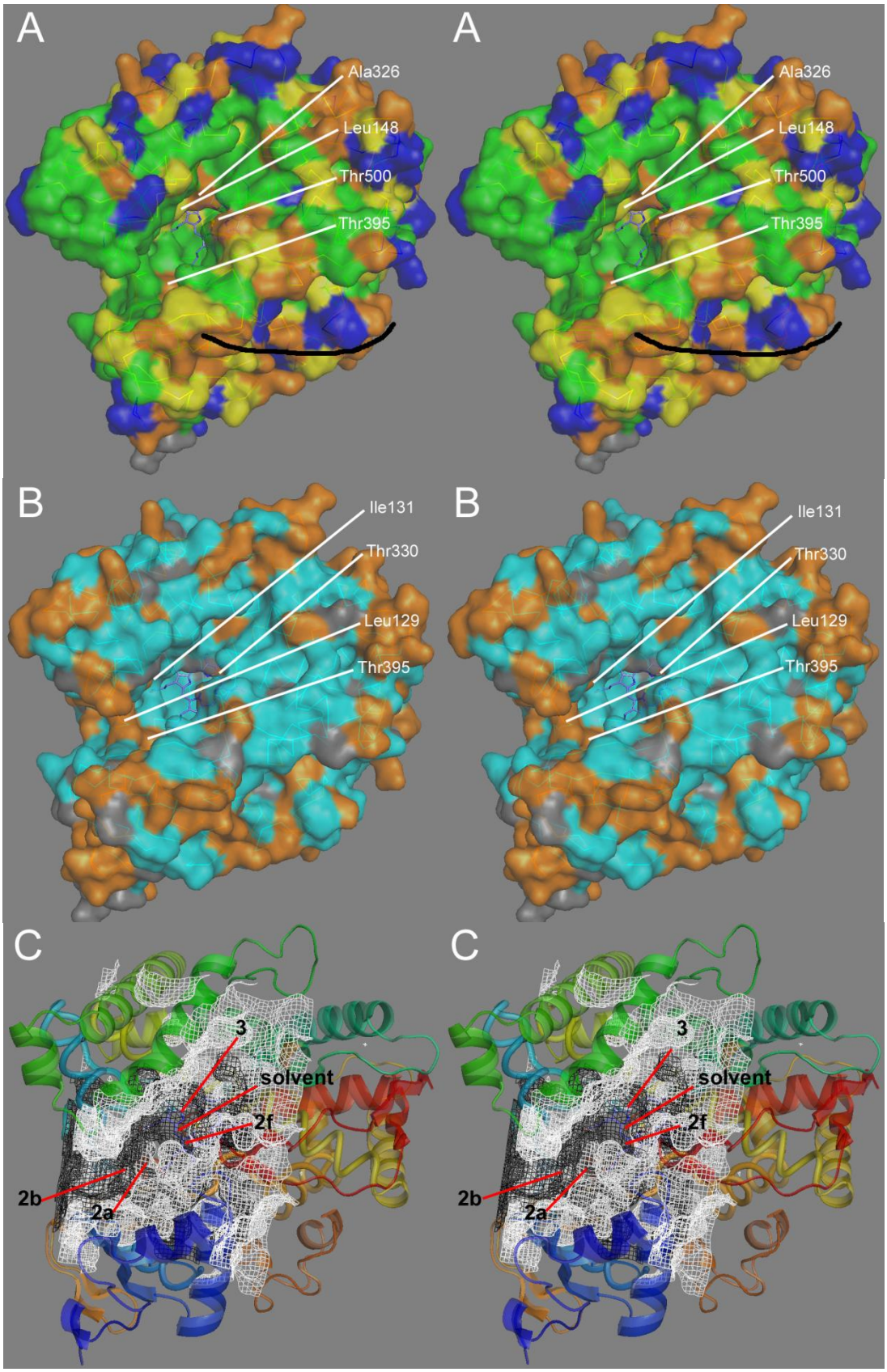

Fig. S1. Stereograms of the rCYP24A1 crystal structure. Panel A shows the degree of conserved residues in 53 species orthologs, >95% green, 80-95% yellow, 60-80% orange, <60% blue. Panel B shows amino acid rotamer variation in two crystal structures (two chains each) with invariant rotamers (cyan), two or more rotamers (orange), and nonrotameric alanine, glycine, and proline (gray). Panel C shows the hCYP24A1 model active site cavity within the rCYP24A1 crystal structure cavity and the orientation of various access channel trajectories: pw2a, pw2b, pw2f, pw3, and solvent channel. Evidence suggests that pw2a operates in CYP24A1.

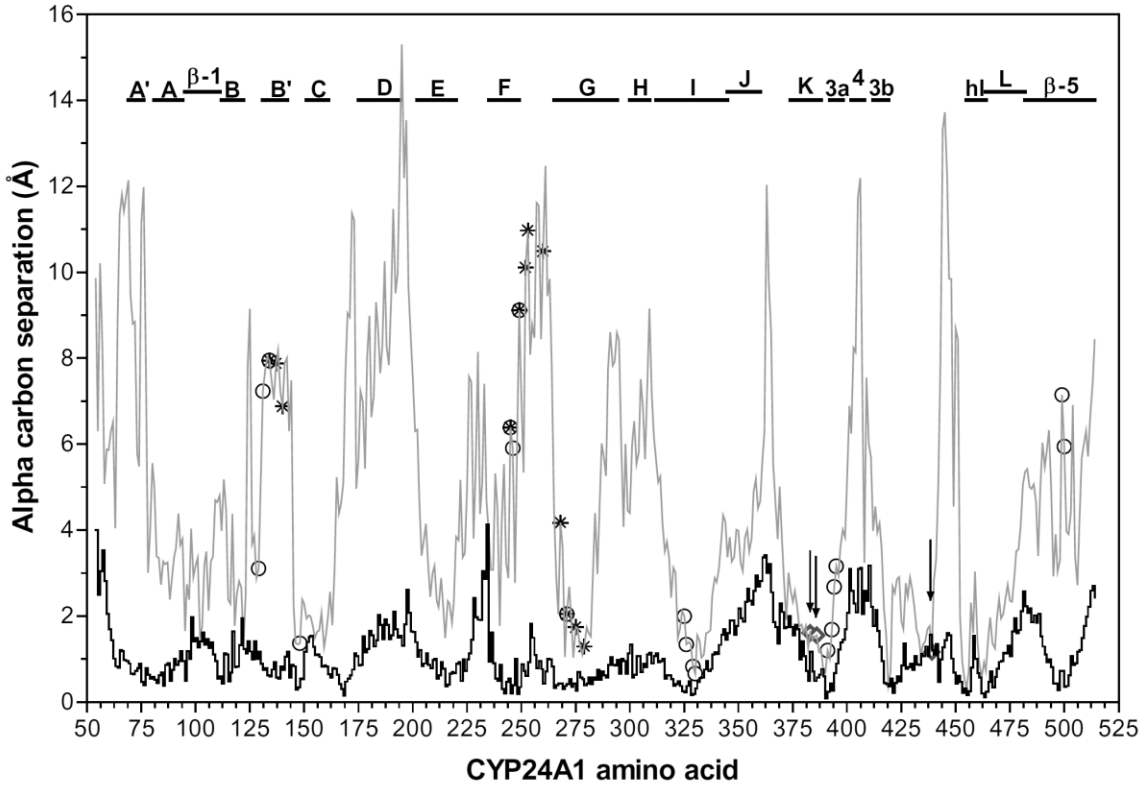

Fig. S2. Alpha carbon separation between rCYP24A1 structures (CHAPS chain A and Cymal-5 chain A; dark line) and CHAPS chain A and a model of hCYP24A1 (grey line). Positions of aromatic cluster residues (*) and active site contact residues (o) and the ERR-triad residues (arrows) are indicated. The average RMSD for CHAPS-Cymal-5 and CHAPS-model were 1.33 Å and 5.56 Å.

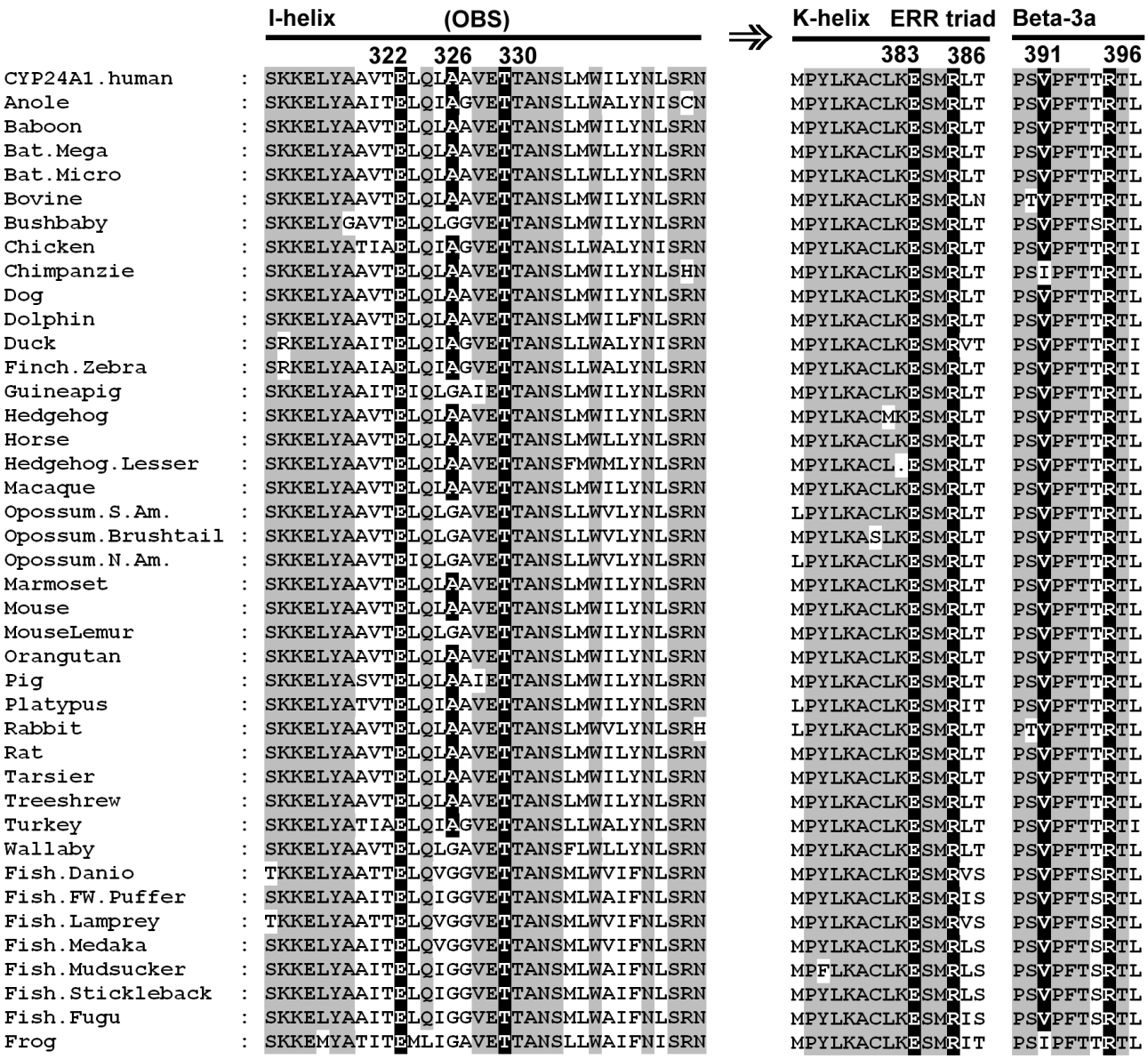

Fig. S3. Partial CYP24A1 sequence alignment of 41 species showing the I- and K-helices and beta-3a strand. Light shaded residues indicate greater than 95% identity. Dark shaded residues indicate the structurally important residues Glu322 (stabilizes contact residue Leu148 in the B'/C loop), Ala326 (position regulating 23- or 24-hydroxylation), Thr330 (stabilizes the Oxygen Binding Site (OBS) in the I-helix), Glu383 and Arg386 (the first two residues in the ERR triad), Val391 (substrate contact residue mutated in this study), and Arg396 (heme A-ring propionate binding residue).

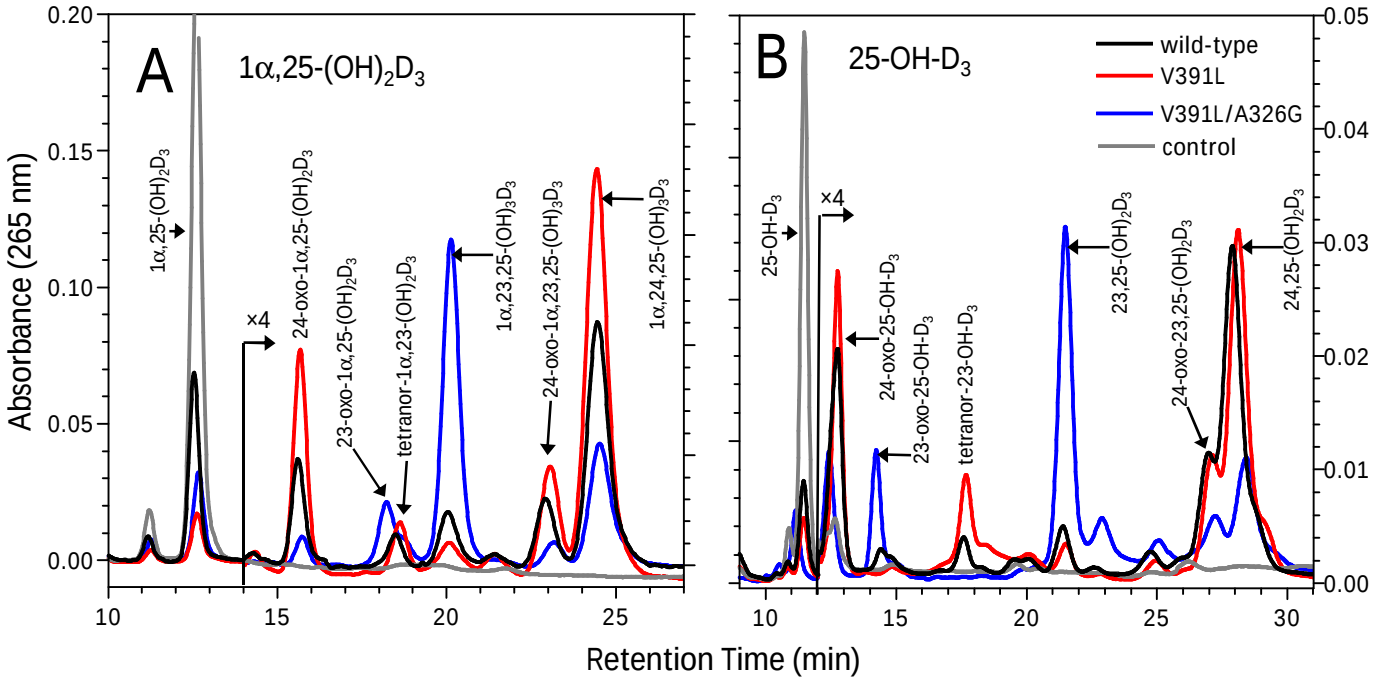

Fig. S4. Metabolism of 25-OH-D_3 by V391L-modified CYP24A1. HPLC profiles of the metabolism of 1a,25-$(OH)_2D_3$ (A) and 25-OH-D_3 (B) by the CYP24A1 mutants under investigation. The legend in panel B, also applies to panel A. The right hand y-axes represent the expanded scale. A quantitative summary of the chromatographic data shown in this figures is presented in Table 1.

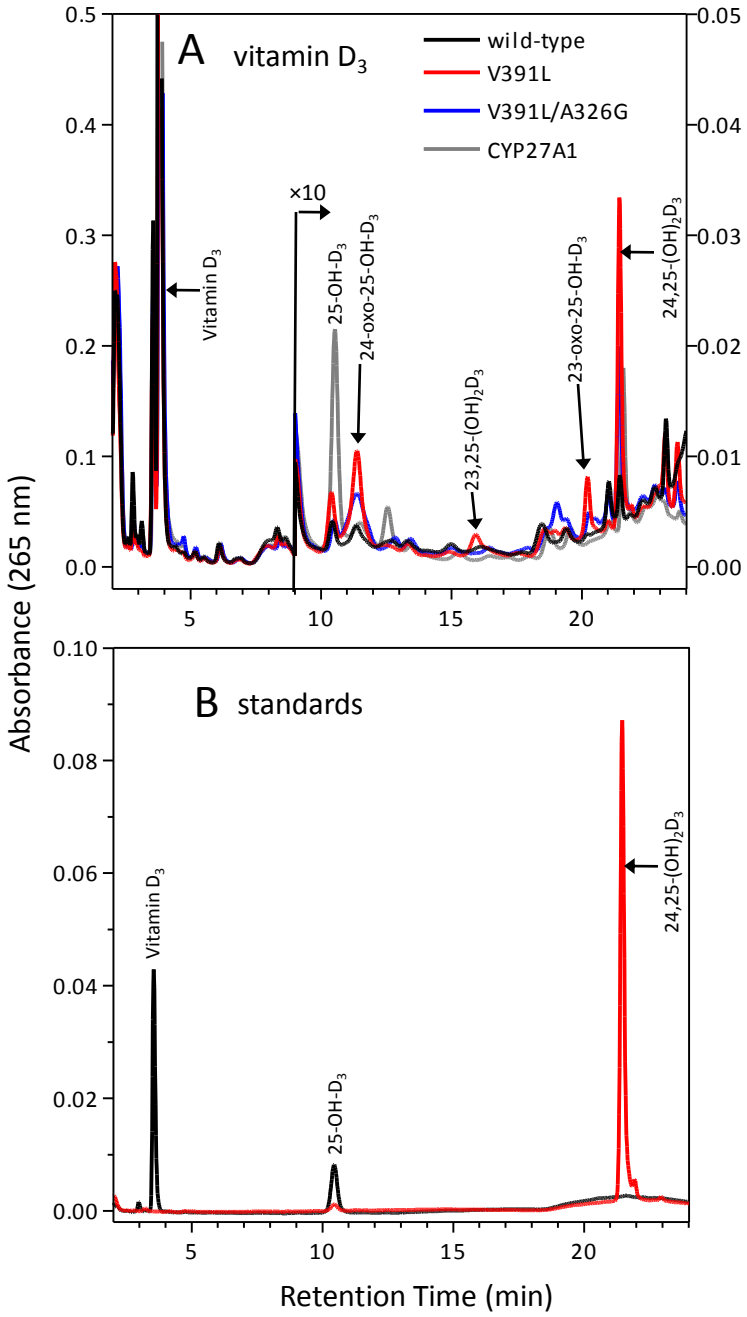

Fig. S5. Metabolism of vitamin D_3 by V391L-modified CYP24A1. HPLC profiles of the metabolism of vitamin D_3 by mutant CYP24A1 and wild-type CYP27A1(A). HPLC analysis of synthetic standards is shown in panel B. The right hand y-axis in A represents the expanded scale.

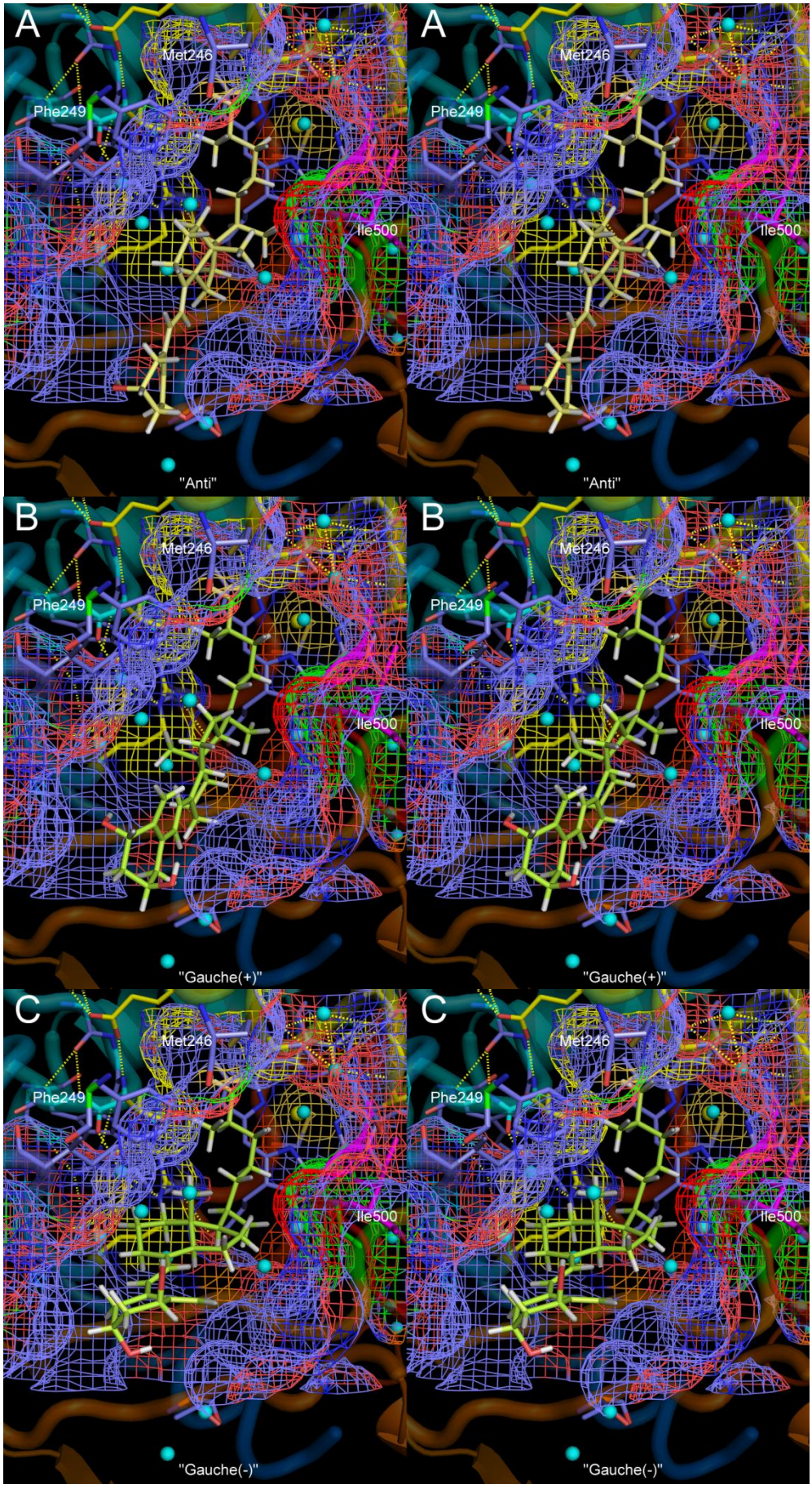

Fig. S6. The docking of the "anti", gauche(+), and gauche(-) conformations of the 1α-OH-D_3 side chain (yellow or green) in the active site cavity of rCYP24A1. These panels illustrate that different conformations of the vitamin D side chain are easily accommodated in the expansive active site cavity of the rCYP24A1 crystal structure. Water molecules are shown as blue spheres.

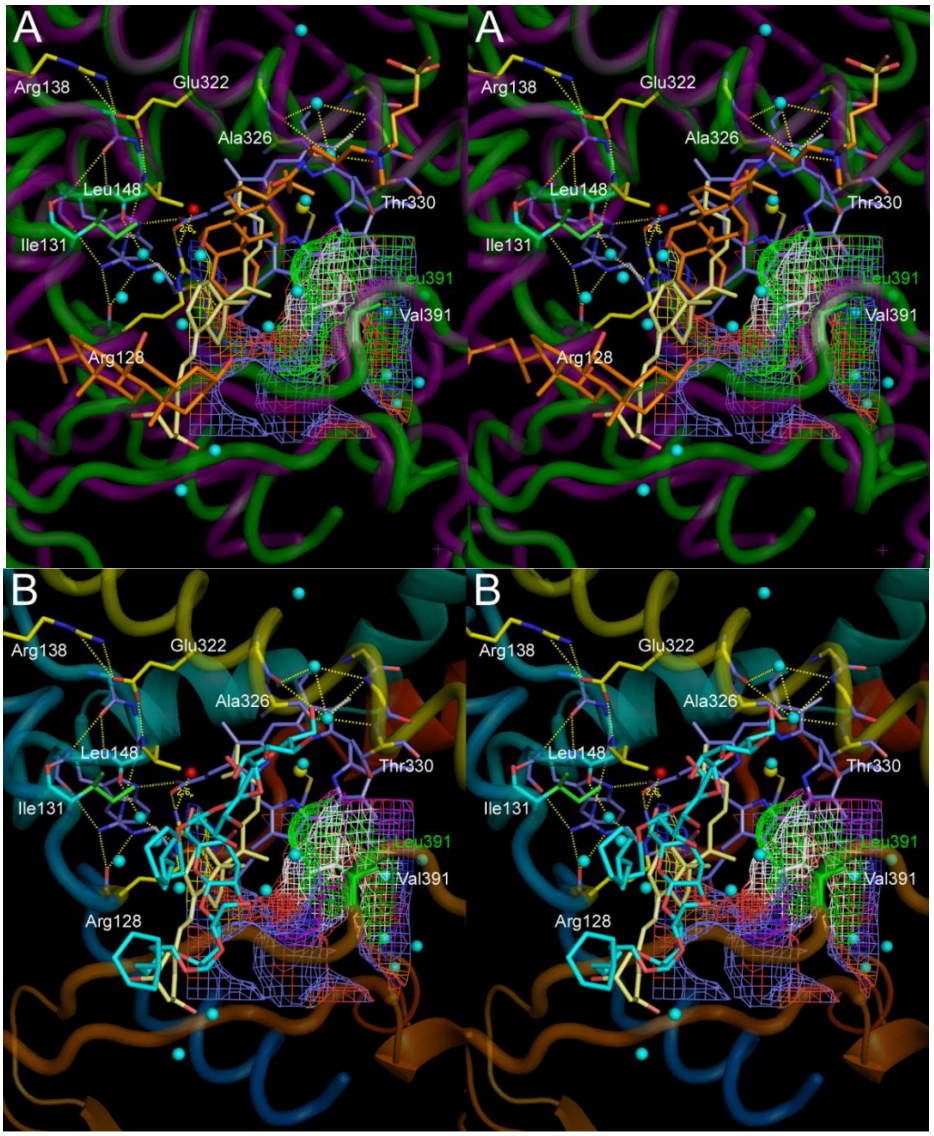

Fig. S7 A-B. Stereograms of regioselectively docked vitamin D structures. Panel A shows the alignment of rCYP24A1 crystal structure (green) with our model of hCYP24A1 (purple) with 1α-OH-D_3 docked for 24-hydroxylation (yellow). The 1α-OH-D_3 is seen to partially overlap with two of the CHAPS surfactant molecules from rCYP24A1 chain A (3k9v.pdb, orange) which occupy non-reactive orientations in the active site. Panel B shows even less overlap with the two Cymol-5 surfactant molecules from rCYP24A1 chain A (3k9y.pdb, cyan) which appear to be oriented in a pw2a access channel trajectory. Water molecules are shown as blue spheres. This figure continues on page S-8.

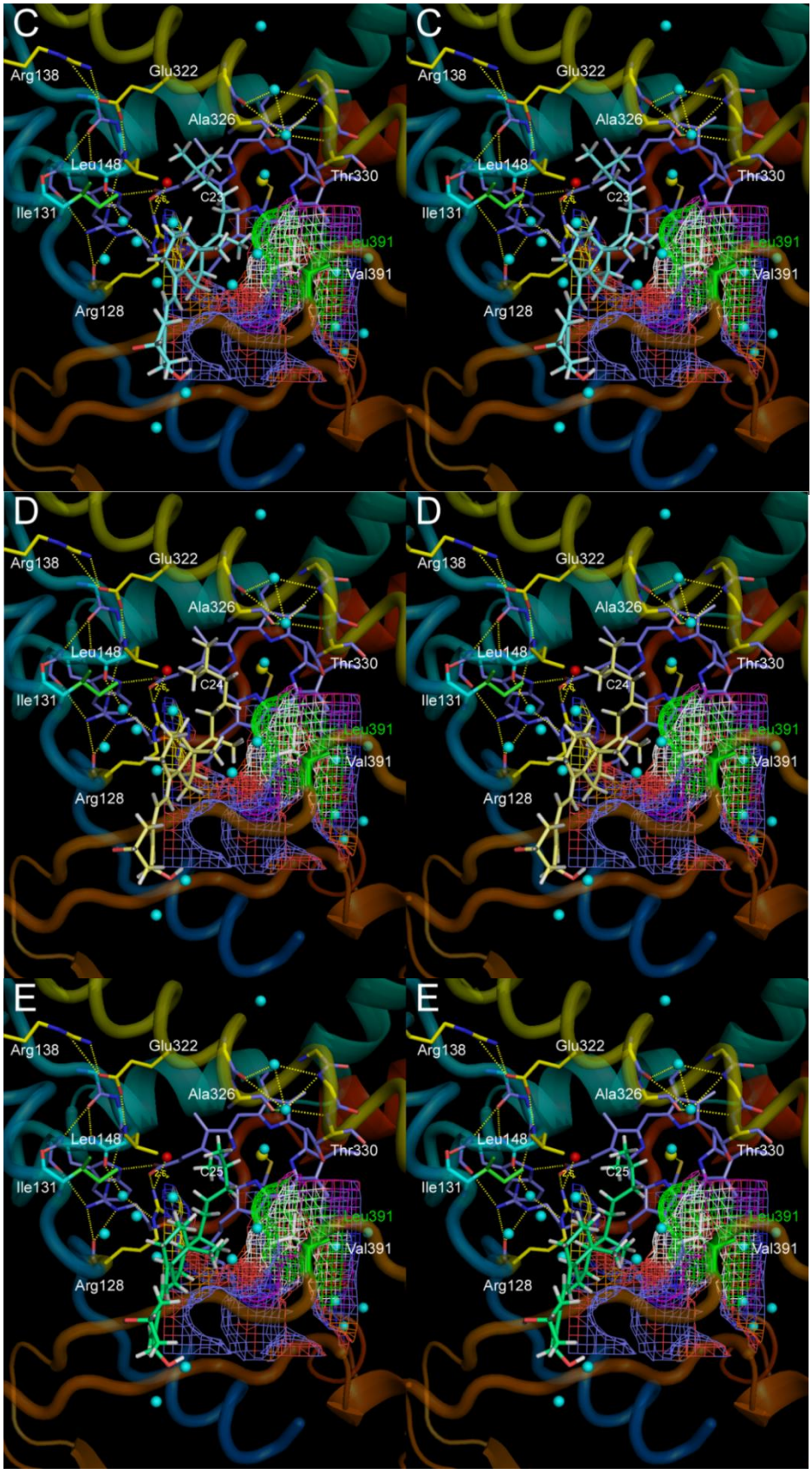

Fig. S7 C-E. Panels C, D, and E allow comparison of 1α-OH-D_3 oriented for 23-, 24-, and 25-hydroxylation, respectively. 1α-OH-D_3 is color-coded for docked orientation: cyan for 23-hydroxylation (C), yellow for 24-hydroxylation (D) and lime green for 25-hydroxylation (E). In each case, there appears to be less conflict between C21 and with the wild-type Val391 (white) and mutant Leu391 (green) surfaces which is consistent with the increased activity of the V391L mutants. Key functional and substrate contact residues are labeled (the rCYP24A1 residue Met148 is replaced by the human ortholog residue Leu148) and the position of a hypothetical water molecule capable of bridging the heme-bound Arg128 to a substrate 25-hydroxyl group is shown as a red sphere near Leu148. All other water molecules are shown as blue spheres. This figure continues on page S-9.

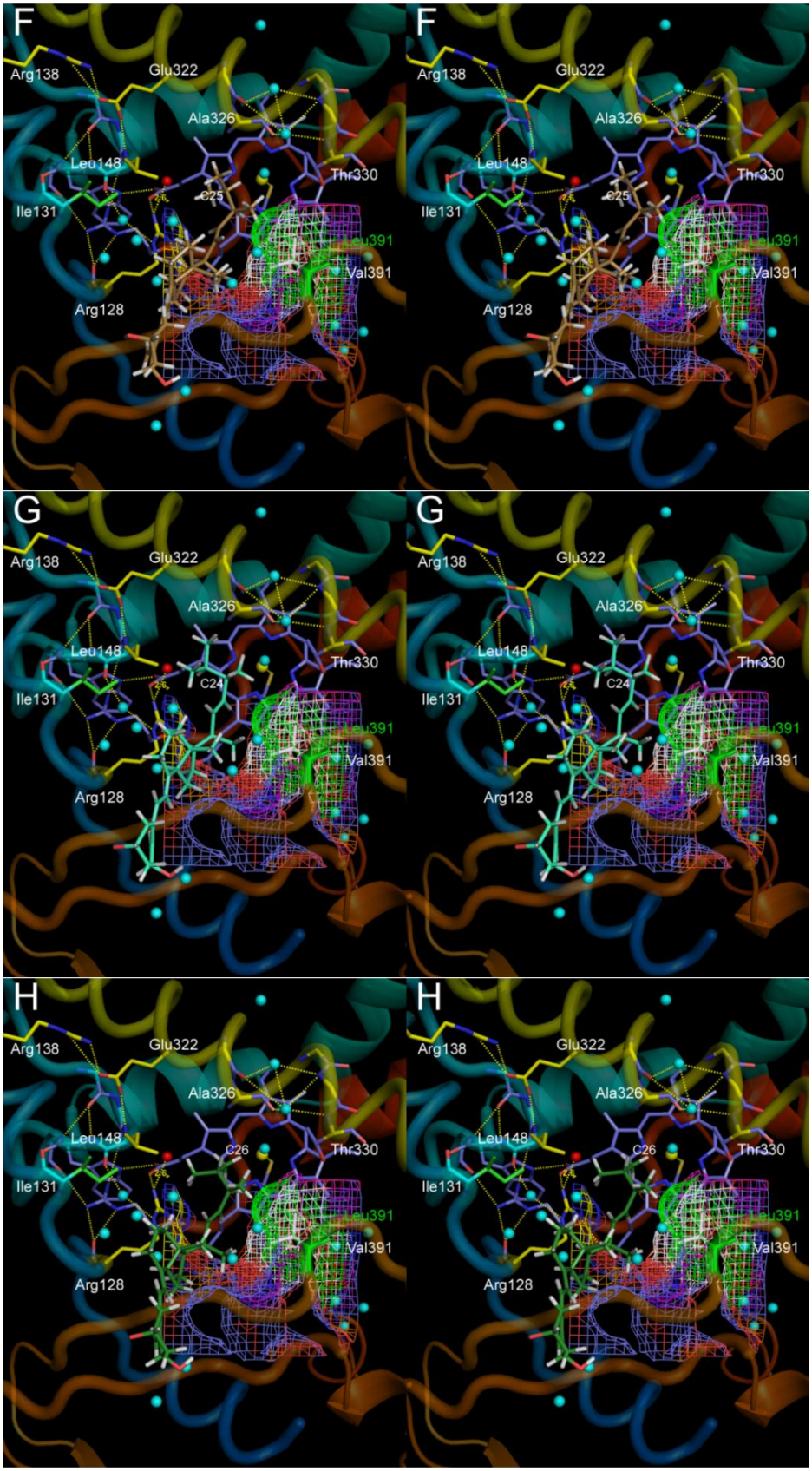

Fig. S7 F-H. Panels F, G and H show 1α-OH-D_2 oriented for 25-, 24-, and 26-hydroxylation respectively. 1α-OH-D_2 is color-coded for docked orientation: brown for 25-hydroxylation (F), cyan for 24-hydroxylation (G) and green for 26-hydroxylation (H). The steric contact of the 24S-methyl group with the Leu391 surface in panel F is consistent with the reduced 25-hydroxylation seen with the V391L, and consistent with the observation of being a better 24- and 26-hydroxylase of 1α-OH-D_2. Water molecules are shown as blue spheres.